



# Prolonged Use of NMDAR Antagonist Develops Analgesic Tolerance in Neuropathic Pain via Nitric Oxide Reduction-Induced GABAergic Disinhibition

Jun Li<sup>1,2</sup> · Lin Zhang<sup>1</sup> · Chu Xu<sup>1</sup> · Yu-Hui Lin<sup>1</sup> · Yu Zhang<sup>1</sup> · Hai-Yin Wu<sup>1</sup> · Lei Chang<sup>1</sup> · Ying-Dong Zhang<sup>3</sup> · Chun-Xia Luo<sup>1</sup> · Fei Li<sup>4</sup> · Dong-Ya Zhu<sup>1,5,6</sup>

Published online: 6 July 2020

© The American Society for Experimental NeuroTherapeutics, Inc. 2020

## Abstract

Neuropathic pain is usually persistent due to maladaptive neuroplasticity-induced central sensitization and, therefore, necessitates long-term treatment. *N*-methyl-D-aspartate receptor (NMDAR)-mediated hypersensitivity in the spinal dorsal horn represents key mechanisms of central sensitization. Short-term use of NMDAR antagonists produces antinociceptive efficacy in animal pain models and in clinical practice by reducing central sensitization. However, how prolonged use of NMDAR antagonists affects central sensitization remains unknown. Surprisingly, we find that prolonged blockage of NMDARs does not prevent but aggravate nerve injury-induced central sensitization and produce analgesic tolerance, mainly due to reduced synaptic inhibition. The disinhibition that results from the continuous decrease in the production of nitric oxide from neuronal nitric oxide synthase, downstream signal of NMDARs, leads to the reduction of GABAergic inhibitory synaptic transmission by upregulating brain-derived neurotrophic factor expression and inhibiting the expression and function of potassium-chloride cotransporter. Together, our findings suggest that chronic blockage of NMDARs develops analgesic tolerance through the neuronal nitric oxide synthase–brain-derived neurotrophic factor–potassium-chloride cotransporter pathway. Thus, preventing the GABAergic disinhibition induced by nitric oxide reduction may be necessary for the long-term maintenance of the analgesic effect of NMDAR antagonists.

**Key Words** Neuropathic pain · NMDA receptors · central sensitization · excitatory/inhibitory synaptic transmission · analgesic tolerance · GABA<sub>A</sub> receptors.

Jun Li and Lin Zhang contributed equally to this work.

**Electronic supplementary material** The online version of this article (<https://doi.org/10.1007/s13311-020-00883-w>) contains supplementary material, which is available to authorized users.

✉ Dong-Ya Zhu  
dyzhu@njmu.edu.cn

<sup>1</sup> Department of Pharmacology, School of Pharmacy, Nanjing Medical University, Nanjing 211166, China

<sup>2</sup> Department of Pharmacy, Nanjing First Hospital, Nanjing Medical University, Nanjing 210006, China

<sup>3</sup> Department of Neurology, Nanjing First Hospital, Nanjing Medical University, Nanjing 210006, China

<sup>4</sup> Department of Medicinal Chemistry, School of Pharmacy, Nanjing Medical University, Nanjing 211166, China

<sup>5</sup> Institution of Stem Cells and Neuroregeneration, Nanjing Medical University, Nanjing 211166, China

<sup>6</sup> Guangdong-Hong Kong-Macao Greater Bay Area Center for Brain Science and Brain-Inspired Intelligence, Guangzhou 510000, China

## Introduction

Neuropathic pain is a painful condition which is a direct consequence of a lesion or disease affecting the somatosensory nervous system [1]. Neuropathic pain can result from various conditions, including postherpetic neuralgia, painful diabetic polyneuropathy, trigeminal neuralgia, multiple sclerosis, HIV infection, spinal cord injury, stroke, and cancer [1, 2]. A best estimate of population prevalence of pain with neuropathic characteristics is likely to lie between 6.9 and 10% [3].

Central sensitization at the spinal level, a prolonged hyperexcitability of dorsal horn nociceptive neurons caused by neural plasticity, is crucial for both the development and maintenance of neuropathic pain [4–6]. Most analgesics used for neuropathic pain affect central sensitization [7]. Nerve injury triggers long-term plastic changes along sensory pathways, from the peripheral sensory terminals to the dorsal horn [8, 9], which determines the persistent nature of neuropathic pain. The persistent nature of neuropathic pain necessitates long-term treatment.

*N*-methyl-D-aspartate receptor (NMDAR)-mediated sensitization in the dorsal horn pain transmission neurons represents key mechanism of central sensitization [4, 10]. Indeed, a variety of NMDAR antagonists produces antinociceptive efficacy in various animal pain models and in clinical practice by reducing central sensitization [11–13]. Central sensitization can also be caused by a loss of  $\gamma$ -aminobutyric acid (GABA)-releasing inhibitory interneurons or a reduction in tonic and phasic inhibitory controls at the spinal level [1, 14, 15]. Peripheral nociceptors project onto excitatory project neurons of lamina I and glutamatergic central transient cells of lamina II<sub>o</sub> in the dorsal horn [16]. GABAergic interneurons are densely innervated in lamina I project neurons to decrease the excitability of lamina I output neurons and modulate pain transmission [17]. Thus, the central sensitization within the spinal cord results from both enhancement of NMDAR-mediated excitatory synaptic transmission (E) and attenuated GABA<sub>A</sub> receptor (GABA<sub>A</sub>R)-mediated inhibitory synaptic transmission (I), that is, dual regulation [18]. Besides, single regulation of E or I alone can change the other because of the interaction between NMDARs and GABA<sub>A</sub>Rs [19, 20]. The frequency of miniature inhibitory postsynaptic currents (mIPSCs) is decreased after blocking NMDARs. On the contrary, the enhancement of GABA<sub>A</sub>Rs by diazepam also causes the enhancement of excitatory synaptic transmission [20]. In accordance with this, experience suggests that highly specific agents that target 1 receptor or channel never progress to the clinic [18]. Therefore, whether prolonged specific blockage of NMDARs can gain long-term relief of neuropathic pain remains doubtful. In this study, we found that chronic use of the NMDAR antagonist MK801 does not reduce but facilitates central sensitization in the dorsal horn, as indicated by decreased inhibitory synaptic transmission and increased excitatory transmission, and leads to analgesic tolerance. The chronic use of MK801-induced potentiation of central sensitization is mainly due to continuous decrease in the production of nitric oxide (NO) from neuronal nitric oxide synthase (nNOS), the downstream signal of NMDARs, thereby reducing GABAergic inhibitory synaptic transmission.

## Materials and Methods

### Experimental Animals

Adult male Sprague-Dawley (250–300 g) rats (from SIPPR-BK, Shanghai, China), adult (6- to 7-week-old) male homozygous nNOS-deficient mice (B6; 129S4-Nos1<sup>tm1Plh</sup>, Nos1<sup>-/-</sup>, stock number: 002633) and their wild-type controls of similar genetic background

(B6129SF2, WT) (both from Jackson Laboratories; maintained at Model Animal Research Center of Nanjing University, Nanjing, China), and male young adult (6- to 7-week-old) C57BL/6 mice (from Model Animal Research Center of Nanjing University, Nanjing, China) were used in this study. The animals were maintained at a controlled temperature (20 ± 2 °C) and group housed (12-h light/dark cycle) with access to food and water *ad libitum*. All procedures involving the use of animals were approved by the Institutional Animal Care and Use Committee of Nanjing Medical University. Every effort was made to minimize the number of animals used and their suffering.

### Neuropathic Pain Model

Neuropathic pain was induced by segmental spinal nerve ligation (SNL). Animals were anesthetized with isoflurane. After the loss of righting reflex, the animal was fixed in the prone position. The SNL model was prepared as described by the method of Chung et al. [21]: a median skin incision with about 3 to 5 cm length in the L4–S2 level of the mouse back was made, the muscles next to the vertebrae till the 6th lumbar protruding were separated, the L5/L6 joint protruding on the right side was exposed and excised, and L6 processus transverse was partially split so that the L4–L6 spinal nerves on the right side were exposed. The L5 nerve was gently isolated and tightly ligated with 5–0 silk thread. The wound was closed with 4–0 silk thread suture and covered with iodine solution. After nerve ligation, animals with signs of paw clonus or autotomy were excluded from further experiments.

### Drugs and Their Administrations

MK801 (Cat#M107) and TrkB-Fc (Cat#T8694) were purchased from Sigma-Aldrich. ANA-12 (Cat#4781) was purchased from Tocris (Bristol, UK). ZL006 was synthesized in our laboratory [22]. Tat-NR2B9C was prepared in our laboratory as described previously [23, 24]. ZL006 was dissolved as described previously [22]. MK801 and TrkB-Fc were dissolved in saline, and ANA-12 was dissolved in DMSO.

**Intrathecal Microinjection** In lightly restrained, unanesthetized mice, a 30G needle attached to a microsyringe was inserted between the L5 and L6 vertebrae, puncturing through the dura (confirmation by the presence of reflexive tail flick), followed by microinjection, as described previously [25].

**Continuous Intrathecal Infusions** Osmotic minipumps (models 1004 for mouse and 2ML4 for rat; Alzet, Cupertino, USA) and intrathecal cannulas (0.61 mm outer diameter and

0.28 mm inner diameter for mouse, 0.99 mm outer diameter and 0.58 mm inner diameter for rat) were filled with a solution of PBS. Cannulas were inserted into the subarachnoid space through the space between the L5 and L6 vertebrae, and the tip of the catheter was implanted at the L5 spinal segmental level [26].

## Behavioral Testing

**Mechanical Nociception Assays** For rats, the threshold for 50% paw withdrawal (50% PWT) response to mechanical stimulus was assessed through dynamic plantar apparatus (Ugo Basile, Italy). The 50% PWT refers to that the probability of paw withdrawal response to repeated mechanical stimulus is 50%. Rats were placed individually in a plastic cage (17 × 15 × 15 cm) with a wire mesh bottom which allowed full access to the paws. Behavioral accommodation was allowed for 15 to 20 min until cage exploration and major grooming activities ceased. A maximal cutoff of 50 g/50 s was set to prevent tissue damage. To record the PWT in response to mechanical stimulus, each rat was measured 5 times with a 5-min interval, and the mean value (the maximal and minimum values excluded) was recorded. The experimental procedures were performed in a double-blind manner.

For mice, the threshold for 50% PWT response to mechanical stimulus was quantified by assessing the paw withdrawal threshold using von Frey filaments (Touch-Test™ Sensory Evaluator, North Coast Medical, Inc.). Mice were placed individually in a plastic cage (4.5 × 5 × 11 cm) with a wire mesh bottom which allowed full access to the paws. Behavioral accommodation was allowed for 20 to 30 min until cage exploration and major grooming activities ceased. Mechanical threshold was measured by applying a von Frey filament to the ventral surface of the right hind paw until a positive sign of pain behavior was elicited. The paradigm for assessing the threshold was as follows. Von Frey filaments with logarithmically incremental stiffness (0.02–2 g) were applied serially to the paw by the up-down method [27]. The filaments were presented, in ascending order of strength, perpendicular to the plantar surface with sufficient force to cause light bending against the paw and held for 4 s. A positive response was noted if the paw was sharply withdrawn. Flinching immediately upon removal of the hair was also considered a positive response. The 2-g filament was selected as the upper limit cutoff for testing. If there was no response at 2-g filament, animals were assigned this cutoff value. The pattern of positive and negative withdrawal responses was converted to 50% threshold according to the formula: 50% PWT = 10 log( $X$ ) +  $\kappa\delta$ .  $X$  = value (in log unit) of the final von Frey hair used,  $\kappa$  is correction factors based on the pattern of responses from

the calibration table, and  $\delta$  = mean difference in log units between stimuli (here, 0.224).

**Thermal Nociception Assays** Paw withdrawal latency response to thermal stimulus was assessed through the Hargreaves test. In the test, infrared heat was applied with a Hargreaves apparatus (Ugo Basile) to the plantar surface of the injured hind paw. Rats were placed individually in a plastic box (17 cm × 15 cm × 15 cm) on a glass platform. Behavioral accommodation was allowed for 15 to 20 min. Radiant heat was shone on the center of the paws and a maximal cutoff of 30 s was set to prevent tissue damage. To record the paw withdrawal latency in response to thermal stimulus, each animal was measured 5 times with a 5-min interval, and the mean value (the maximal and minimum values excluded) was recorded. The experimental procedures were performed in a double-blind manner.

## Electrophysiology

**Electrophysiology Recordings from the Acute Spinal Cord Slices** After anesthetized by ethyl ether, rats (7- to 8-week-old) or mice (6- to 7-week-old) were transcardially perfused with ice-cold cutting solution (in mM, choline chloride 110.0, glucose 20.0, KCl 2.5, CaCl<sub>2</sub> 0.5, MgCl<sub>2</sub> 7.0, NaH<sub>2</sub>PO<sub>4</sub> 1.3, NaHCO<sub>3</sub> 25.0, Na-ascorbate 1.3, Na-pyruvate 0.6) and decapitated. Lumbar spinal cord (L4 and L5) was rapidly removed, and 350 μm cortical slices or 300 μm transverse spinal cord (embedded in a 3% agarose block) slices were made in ice-cold cutting solution using a vibratome (VT1000s, Leica, Germany), neurons were viewed under upright microscopy (Olympus X51W, Tokyo, Japan). Whole-cell recordings from slices were performed at 30 °C with standard intrapipette solution (in mM: Cs-gluconate 132.5, CsCl 17.5, MgCl<sub>2</sub> 2.0, EGTA 0.5, HEPES 10.0, ATP 4.0, QX-314 5.0) in normal ACSF artificial cerebrospinal fluid (in mM: glucose 10.0, NaCl 125, KCl 2.5, CaCl<sub>2</sub> 2, MgCl<sub>2</sub> 1.3, NaH<sub>2</sub>PO<sub>4</sub> 1.3, NaHCO<sub>3</sub> 25.0, Na-ascorbate 1.3, Na-pyruvate 0.6). All solution was bubbled with 95% O<sub>2</sub>–5% CO<sub>2</sub>.

For GABA-evoked current recording, neurons of spinal cord slices were viewed under upright microscopy (Olympus X51W, Nomasky), and standard intrapipette solution (in mM: Cs-gluconate 132.5, CsCl 17.5, MgCl<sub>2</sub> 2.0, EGTA 0.5, HEPES 10.0, ATP 4.0, QX-314 5.0) was used, and GABA was applied to the recorded cell using a manually controlled pulse (4–6 s) of a low subsaturating GABA concentration. Drugs dissolved in DMSO and subsequently diluted with recording solution were co-applied together with GABA without preincubation. Recordings in which access resistance or capacitance changed by 20% during the experiment were excluded from data analysis. One neuron was recorded per slice, and no more than 5 slices were recorded per rat. Each set of experiments was repeated using at least 4 rats. Data were acquired using a Multiclamp 700B amplifier and filtered during acquisition with a low-pass

filter set at 2 kHz and sampled at 10 kHz using pClamp 10.3 (Molecular Devices). Data analysis was performed offline with Clampfit 10.2 (Molecular Devices).

For NMDA-induced currents recording, ACSF artificial cerebrospinal fluid (in mM: NaCl 117, KCl 3.6, CaCl<sub>2</sub> 2.5, MgCl<sub>2</sub> 1.2, NaH<sub>2</sub>PO<sub>4</sub> 1.2, NaHCO<sub>3</sub> 25.0, glucose 11.5) and pipette solution (K-gluconate 135, CaCl<sub>2</sub> 0.5, MgCl<sub>2</sub> 2, KCl 5, EGTA 5, HEPES 5, D-glucose 5, ATP-Mg salt 5, and QX-314 5) were used. The membrane potential was held at -40 mV. TTX (0.5 μM) was presented in the bath solution, and 50 μM NMDA was used to induce the currents.

For miniature postsynaptic current (mPSC) measurements, whole-cell recordings were made from putative excitatory neurons in superficial dorsal horn laminae I using low-resistance pipettes (4–8 MΩ). Before mPSC measurements, excitatory neurons were distinguished from inhibitory neurons by firing pattern analysis according to the established relationship between neuronal firing pattern and its neurotransmitter phenotype [28–30]. Action potential firing was evoked by repeated depolarizing current injections of 1000 ms duration with step-wise increasing amplitudes (-20 to +200 pA) in current-clamp mode. For miniature excitatory postsynaptic current (mEPSC) measurement, the membrane potential was held at -60 mV. Intrapipette solution containing Cs-gluconate 32.5, CsCl 17.5, MgCl<sub>2</sub> 2.0, EGTA 0.5, HEPES 10.0, ATP 4.0, and QX-314 5.0 (in mM) was used. Tetrodotoxin (0.5 μM) and bicuculline (20 μM) were added to block action potentials and GABA<sub>A</sub> receptor-mediated currents, respectively. For mIPSC measurement, the membrane potential was held at -70 mV, and microelectrodes were filled with internal pipette solution containing CsCl 140, HEPES 10.0, MgATP 4.0, NaGTP 3.0, EGTA 1.0, MgCl<sub>2</sub> 1.0, and CaCl<sub>2</sub> 0.3 (in mM). To isolate mIPSCs, tetrodotoxin (0.5 μM), NBQX (10 μM), and APV (50 μM) were present. Recordings in which access resistance or capacitance changed by 20% during the experiment were excluded from data analysis. One neuron was recorded per slice, and no more than 4 slices were recorded per rat. Each set of experiments was repeated using 12 neurons from 4 to 6 animals. Each recording lasts more than 5 min. Data were analyzed using Mini software. Up to 120 events from each neuron were selected at a fixed sampling interval to generate cumulative probability. Data were acquired using a Multiclamp 700B amplifier and filtered during acquisition with a low-pass filter set at 2 kHz and sampled at 10 kHz using pClamp 10.3 (Molecular Devices).

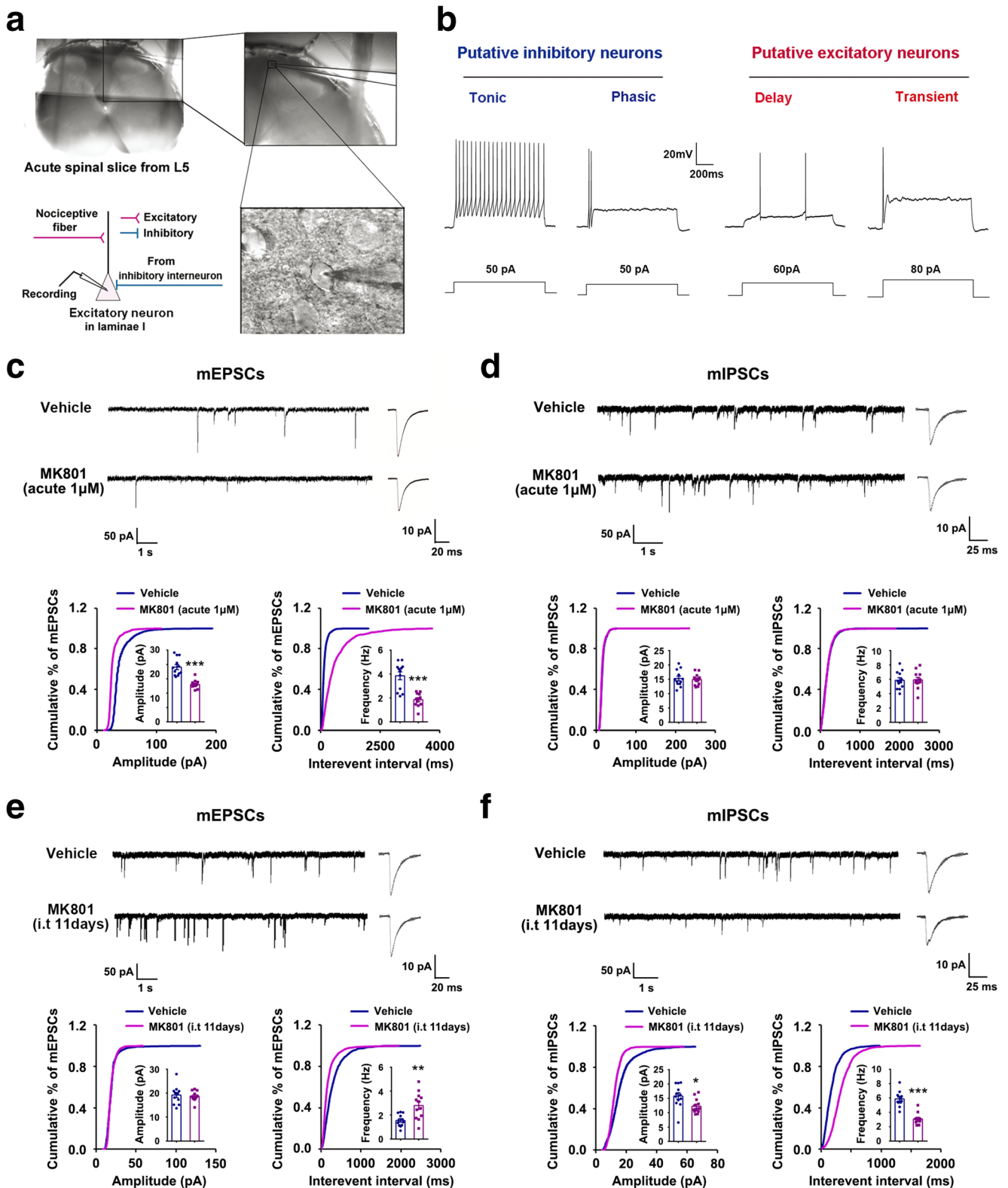
**Estimation of EC<sub>50</sub> and E<sub>max</sub>** EC<sub>50</sub> and E<sub>max</sub> values were estimated by fitting concentration–response curves to the Hill equation according to the following formula:  $I = I_{\max} / (1 + [EC_{50}/(A)]^h)$  as described previously [31].

**Fig. 1** Prolonged blockage of NMDARs induces central sensitization at the spinal level. (a) Images showing the spinal dorsal horn and whole-cell patch-clamp recordings from neurons of laminae I in the dorsal horn. (b) Action potential firing pattern of putative excitatory and inhibitory neurons in the spinal cord dorsal horn. (c–f) Recordings of mIPSCs and mEPSCs. Upper, representative (left) and averaged (right) traces of mPSCs. Lower, cumulative distribution plots and bar graph showing amplitude (left) and frequency (right) of mPSCs. (c) Recordings of mEPSCs from acute spinal slices of rats incubated with MK801 (1 μM) or vehicle for 30 min (for amplitude,  $F(1, 22) = 6.187$ , vehicle vs MK801 (1 μM):  $***p < 0.001$ ; for frequency,  $F(1, 22) = 8.687$ ,  $***p < 0.001$ , 2-tailed  $t$  test,  $n = 12$ ). (d) Recordings of mIPSCs from acute spinal slices of rats incubated with MK801 (1 μM) or vehicle for 30 min (for amplitude,  $F(1, 22) = 0.372$ ,  $p = 0.713$ ; for frequency,  $F(1, 22) = 0.123$ ,  $p = 0.903$ , 2-tailed  $t$  test,  $n = 12$ ). (e) Recordings of mEPSCs from acute spinal slices of rats that received intrathecal infusion of MK801 (5 μg/day, ×11 days) (for amplitude,  $F(1, 22) = 0.394$ ,  $p = 0.698$ ; for frequency,  $F(1, 22) = 3.49$ ,  $**p = 0.002$ , 2-tailed  $t$  test,  $n = 12$ ). (f) Recordings of mIPSCs from acute spinal slices of rats that received intrathecal infusion of MK801 (5 μg/day × 11 days) (for amplitude,  $F(1, 22) = 2.627$ ,  $*p = 0.016$ ; for frequency,  $F(1, 22) = 7.441$ ,  $***p < 0.001$ , 2-tailed  $t$  test,  $n = 12$ ). All data are shown as mean ± SEM

Here,  $I$  is the peak current at a given concentration of agonist  $A$ ,  $I_{\max}$  is the maximum current,  $EC_{50}$  is the concentration of agonist yielding a half maximal current, and  $h$  is the Hill coefficient. Data analysis was performed offline with Clampfit 10.2 (Molecular Devices) and OriginPro 9.4 (OriginLab).

## Tissue Isolation and Western Blot Analysis

Western blot analysis was performed as described previously [23]. Briefly, the dorsal spinal cord (L4 and L5) was dissected from sham or SNL rats and homogenized in 400 μl RIPA lysis buffer containing 1 μM pepstatin, 10 μg/ml aprotinin, 10 μg/ml leupeptin, and 10 μM phenylmethylsulfonyl fluoride. After lysis for 30 min in ice, samples were centrifuged at 12,000×g for 15 min. The protein content in each supernatant fraction was determined by using Bradford's solution, and samples containing equivalent amounts of protein were applied to 10% or 15% (10% for potassium-chloride cotransporter (KCC2) and phosphorylated KCC2 (pKCC2), 15% for brain-derived neurotrophic factor (BDNF)) acrylamide denaturing gels (SDS-PAGE). The separated proteins were transferred onto a polyvinylidene fluoride membrane. The primary antibodies were as follows: rabbit anti-KCC2 (1:2000; Millipore 07-432, RRID:AB\_310611), rabbit anti-pKCC2 (1:1000; Novus NBP2-29513), and rabbit anti-BDNF (1:1000; Thermo PA1-18357, RRID:AB\_1070634). Internal control was performed using rabbit anti-β-actin (1:1000; Bioss bs-0061R, RRID:AB\_10855480). Appropriate horseradish peroxidase-linked secondary antibodies were used for detection by enhanced chemiluminescence (Bio-Rad).



## Quantification and Statistical Analysis

All data are presented as means  $\pm$  SEM. Comparisons among multiple groups were made with 1-way ANOVA (1 factor)

followed by Scheffe's post hoc test or 2-way repeated measures ANOVA (2 factors) followed by Bonferroni's post hoc test. Comparisons between 2 groups were made with a 2-tailed Student's *t* test. Statistical significance was set at

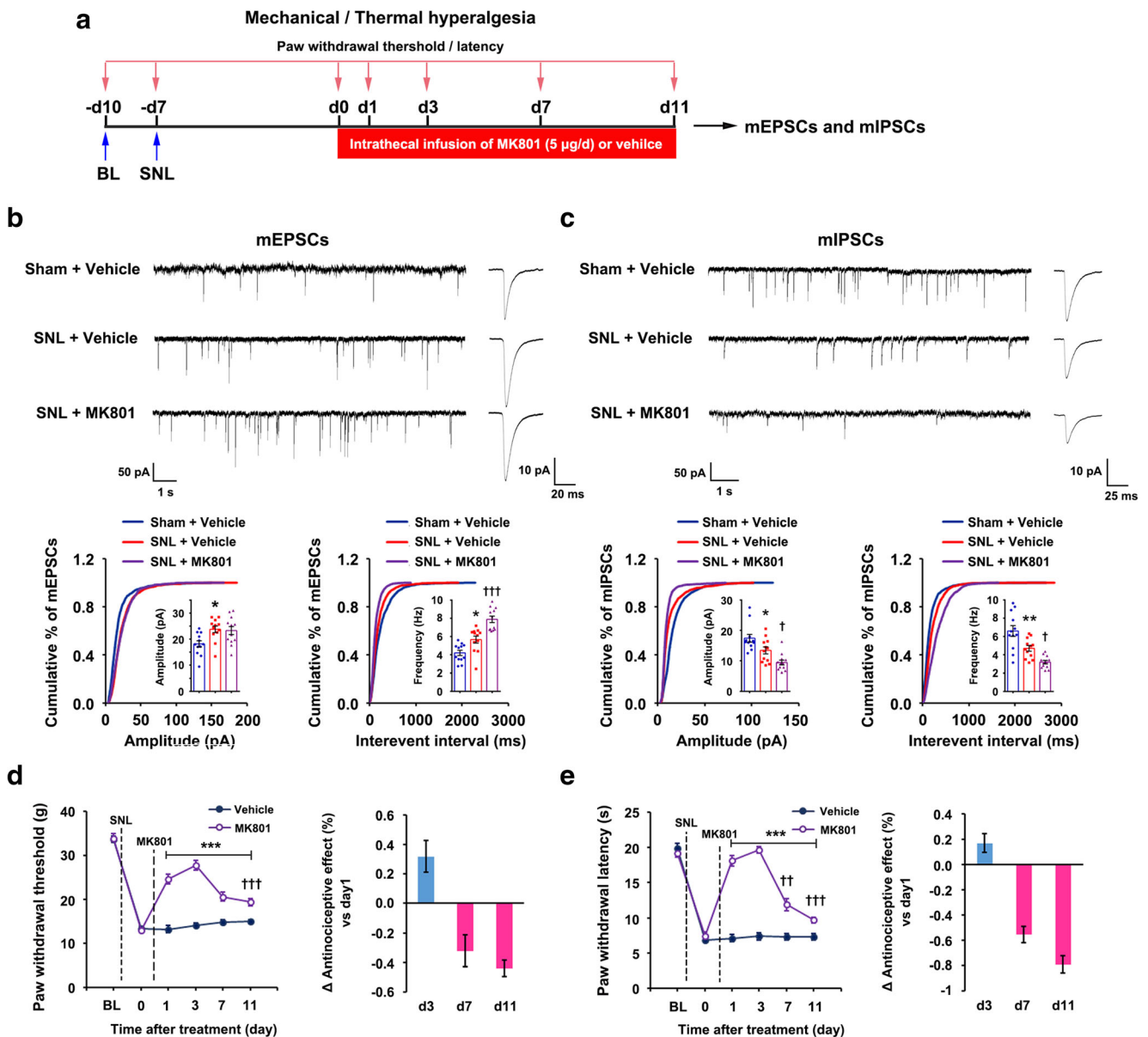


**Fig. 2** Prolonged blockage of NMDARs aggravates SNL-induced E-I imbalance in the dorsal horn and leads to analgesic tolerance. **(a)** Design of the experiments for **(b–e)**. **(b–c)** Recordings of mEPSCs **(b)** and mIPSCs **(c)** from acute spinal slices of rats undergoing SNL surgery and treated with MK801 (5 µg/day × 11 days, per animal) or vehicle. Upper, representative (left) and averaged (right) traces of mPSCs. Lower, cumulative distribution plots and bar graph showing the amplitude (left) and frequency (right) of mPSCs. In **(b)**, for amplitude,  $F(2, 33) = 5.303$ , sham versus SNL:  $*p = 0.022$ ; for frequency,  $F(2, 33) = 28.969$ , sham versus vehicle:  $*p = 0.019$ , MK801 versus vehicle:  $†††p = 0.0003$ , 1-way ANOVA,  $n = 12$ . In **(c)**, for amplitude,  $F(2, 33) = 13.567$ , sham versus vehicle:  $*p = 0.045$ , MK801 versus vehicle:  $†p = 0.046$ ; for frequency,  $F(2, 33) = 18.076$ , sham versus vehicle:  $*p = 0.008$ , MK801 versus vehicle:  $†p = 0.041$ , 1-way ANOVA,

$n = 12$ . **(d)** Left, mechanical hyperalgesia expressed as paw withdrawal threshold of rats subjected to SNL surgery and treated with MK801 (5 µg/day × 11 days, per animal) or vehicle ( $F(1, 23) = 100.69$ , between groups,  $***p < 0.001$ ; within group,  $†††p = 0.0009$  (day 11 vs day 1), repeated measurements ANOVA,  $n = 12-13$ ). Right, the percent change of thermal threshold for each subject. **(e)** Left, thermal hyperalgesia expressed as paw withdrawal latency of rats subjected to SNL surgery and treated with MK801 (5 µg/day × 11 days, per animal) or vehicle ( $F(1, 22) = 130.18$ , between groups,  $***p = 0.001$ , within group,  $††p = 0.002$  (day 7 vs day 1),  $†††p < 0.001$  (day 11 vs day 1), repeated measurements ANOVA,  $n = 12$ ). Right, the percent change of thermal threshold for each subject. BL = baseline. All data are shown as mean ± SEM

$p < 0.05$ . The sample size was predetermined by analyzing pre-experimental data with PASS (power analysis and sample size) software. For animal studies, the sample size was

predetermined by our prior experience. Randomization was used in all experiments. Investigators were blind to the treatment group when assessing the outcome.

## Results

### Prolonged Blockage of NMDARs Aggravates Nerve Injury-Induced Central Sensitization and Produces Analgesic Tolerance

Based on the crucial role of NMDARs in the central sensitization [4], we studied whether short-term and long-term exposures of NMDAR antagonists have different effects on synaptic transmission in the spinal dorsal horn. We intrathecally infused MK801, a noncompetitive antagonist of NMDARs, for 1 day or 11 consecutive days (5  $\mu\text{g}/\text{day}$ ) using osmotic pump into the vertebral column of rats and measured mEPSCs and mIPSCs in putative excitatory neurons of superficial laminae I in the dorsal horn (Fig. 1a) that receive noxious inputs [16]. Excitatory neurons were distinguished from inhibitory neurons by firing pattern analysis according to the established relationship between neuronal firing pattern and its neurotransmitter phenotype [28–30] (Fig. 1b). Confusingly, intrathecal administration with MK801 for 1 day had no effect on either mEPSCs or mIPSCs (Fig. S1). This may be due to the fact that with the withdrawal of MK801, its effect on NMDARs gradually declined and disappeared overtime because of the short half-life of MK801 of the elimination phase and continuous wash-out [32, 33]. To show the acute effect of MK801 on blocking NMDARs, we chose to incubate spinal slices with MK801 for 30 min as this method of drug administration was close to intrathecal delivery. As expected, exposure of slices to MK801 for 30 min *in vitro* significantly decreased the amplitude and frequency of mEPSCs (Fig. 1c) although had no effect on mIPSCs (Fig. 1d), indicating substantially reduced excitatory synaptic transmission. Surprisingly, however, chronic intrathecal infusion of MK801 significantly increased mEPSC frequency (Fig. 1e) and decreased the amplitude and frequency of mIPSCs (Fig. 1f). These data suggest that chronic blockage of NMDARs impairs inhibitory synaptic transmission and enhances excitatory synaptic transmission in the dorsal horn. To study whether the reactivity of NMDARs to MK801 changes after long-term blockage, we tested the NMDA-induced currents after intrathecal infusion of MK801 for 1 day or 11 days and found that 1  $\mu\text{M}$  MK801 still showed potent blocking effect on NMDARs after 11 days of MK801 treatment (Fig. S2). Moreover, after long-term blockage of NMDARs, the amplitude of 10  $\mu\text{M}$  NMDA-induced currents was similar to that after 1 day treatment of MK801, indicating the function of NMDARs in the spinal dorsal horn was not significantly changed.

To determine whether chronic blockage of NMDARs under neuropathic pain conditions causes E–I imbalance, we subjected rats to segmental SNL, a neuropathic pain model in rodents [21]. We intrathecally infused MK801 (5  $\mu\text{g}/\text{day}$ ) or vehicle for 11 consecutive days using

osmotic pump into the vertebral column of rats and measured mEPSCs and mIPSCs in putative excitatory neurons of laminae I (Fig. 2a). SNL surgery significantly increased the amplitude and frequency of mEPSCs (Fig. 2b) and decreased the amplitude and frequency of mIPSCs (Fig. 2c), compared with sham with vehicle, suggesting that peripheral nerve injury causes central sensitization in the dorsal horn. Very surprisingly, chronic intrathecal infusion of MK801 aggravated the SNL-induced central sensitization in the dorsal horn, as the treatment further significantly increased the frequency of mEPSCs (Fig. 2b) and significantly decreased the amplitude and frequency of mIPSCs (Fig. 2c), compared with the SNL with vehicle. Together, chronic blockage of NMDARs leads to central sensitization, especially disinhibition in the dorsal horn.

Next, we studied whether chronic use of the NMDAR antagonist can get long-term relief of neuropathic pain. We intravenously injected MK801 (0.25 mg/kg/day) for 11 consecutive days to the rats subjected to SNL and measured SNL-induced mechanical hyperalgesia. Consistent with its aggravating SNL-induced central sensitization, the chronic use of MK801 caused a significant analgesic tolerance, as indicated by its efficacy that significantly decreased over time (Fig. 2d). To further confirm the finding, we administered MK801 by intrathecal infusion into the vertebral column using osmotic pump and measured SNL-induced thermal pain in rats. Similarly, the chronic infusion of MK801 (5  $\mu\text{g}/\text{day}$ ,  $\times$  11 days) also produced analgesic tolerance in thermal pain (Fig. 2e). Therefore, chronic blockage of NMDARs leads to central sensitization at the spinal level and to analgesic tolerance.

### Reduced Activation of nNOS Accounts for the Chronic Blockage of NMDAR-Induced Disinhibition and Analgesic Tolerance

To know how the chronic blockage of NMDARs leads to disinhibition in the dorsal horn, we focused on the downstream signal of NMDAR activation, NO production through the association of neuronal NO synthase (nNOS) to scaffolding protein postsynaptic density-95 (PSD-95) [22]. We detected the effect of ZL006, a small molecule disruptor of PSD-95–nNOS coupling that is effective in attenuating chronic pain [11, 34], on mIPSCs and mEPSCs in putative excitatory neurons of laminae I in the dorsal horn. Exposure of slices to ZL006 (1  $\mu\text{M}$ ) for 30 min *in vitro* had no effect on mIPSCs (Fig. 3a) and mEPSCs (Fig. 3b), compared with vehicle. However, chronic intrathecal infusion of ZL006 into the vertebral column of rats using osmotic pump for 11 consecutive days (0.2 mg/day, per animal) significantly decreased mIPSC frequency and amplitude in the acute spinal slices (Fig. 3c) and had no effect on mEPSCs (Fig. 3d), compared with vehicle. Next, we injected ZL006 (10 mg/kg/day, *i.v.*,  $\times$  11 days)

into the rats subjected to SNL and measured mechanical and thermal hyperalgesia (Fig. 3e). Similar to the chronic use of MK801, the chronic use of ZL006 showed significant analgesic tolerance on rats (Fig. 3f). Moreover, the chronic use of ZL006 also produced analgesic tolerance on rats in thermal pain (Fig. 3g). Therefore, chronically dissociating nNOS from PSD-95 leads to disinhibition at the spinal level and to analgesic tolerance.

Tat-NR2B9C is a peptide that reduces NMDAR-mediated NO production by dissociating PSD-95 from NMDARs [35]. Accordingly, we observed the effect of Tat-NR2B9C on mIPSCs and mEPSCs in putative excitatory neurons of laminae I in the dorsal horn. Similar with ZL006, exposure of slices to Tat-NR2B9C (100 nM) for 30 min *in vitro* had no effect on mEPSCs nor mIPSCs (Fig. 4 c and d), compared with vehicle. However, chronic use of Tat-NR2B9C (intrathecal microinjection in mice for 11 consecutive days, 0.5 pM/day, per animal) significantly decreased mIPSC frequency and amplitude in the acute spinal slices (Fig. 4 e and f).

To further determine the role of neuronal NO synthase in the chronic blockage of NMDAR-induced disinhibition, we detected the effect of MK801 on synaptic transmission in putative excitatory neurons of laminae I in the dorsal horn in nNOS knockout (KO) and wild-type (WT) mice. Consistent with the results from rats, chronic intrathecal infusion of MK801 (2 µg/day, × 11 day) using osmotic pump into the vertebral column of WT mice significantly increased mEPSC frequency (Fig. 5 a and b) and significantly decreased amplitude and frequency of mIPSCs (Fig. 5 c and d), compared with vehicle. The same as in WT mice, the chronic intrathecal infusion of MK801 significantly increased mEPSCs frequency also in nNOS KO mice (Fig. 5 a and b), compared with vehicle, suggesting that the PSD-95–nNOS–NO cascade is not involved in the enhancement of excitatory synaptic transmission by chronic blockage of NMDARs. However, in nNOS KO mice, the chronic intrathecal infusion of MK801 had no effect on mIPSCs (Fig. 5 c and d), implicating PSD-95–nNOS–NO cascade in the chronic blockage of NMDAR-induced disinhibition.

### Analgesic Tolerance of MK801 Results from GABA<sub>A</sub>R Dysfunction Through the BDNF–KCC2 Pathway

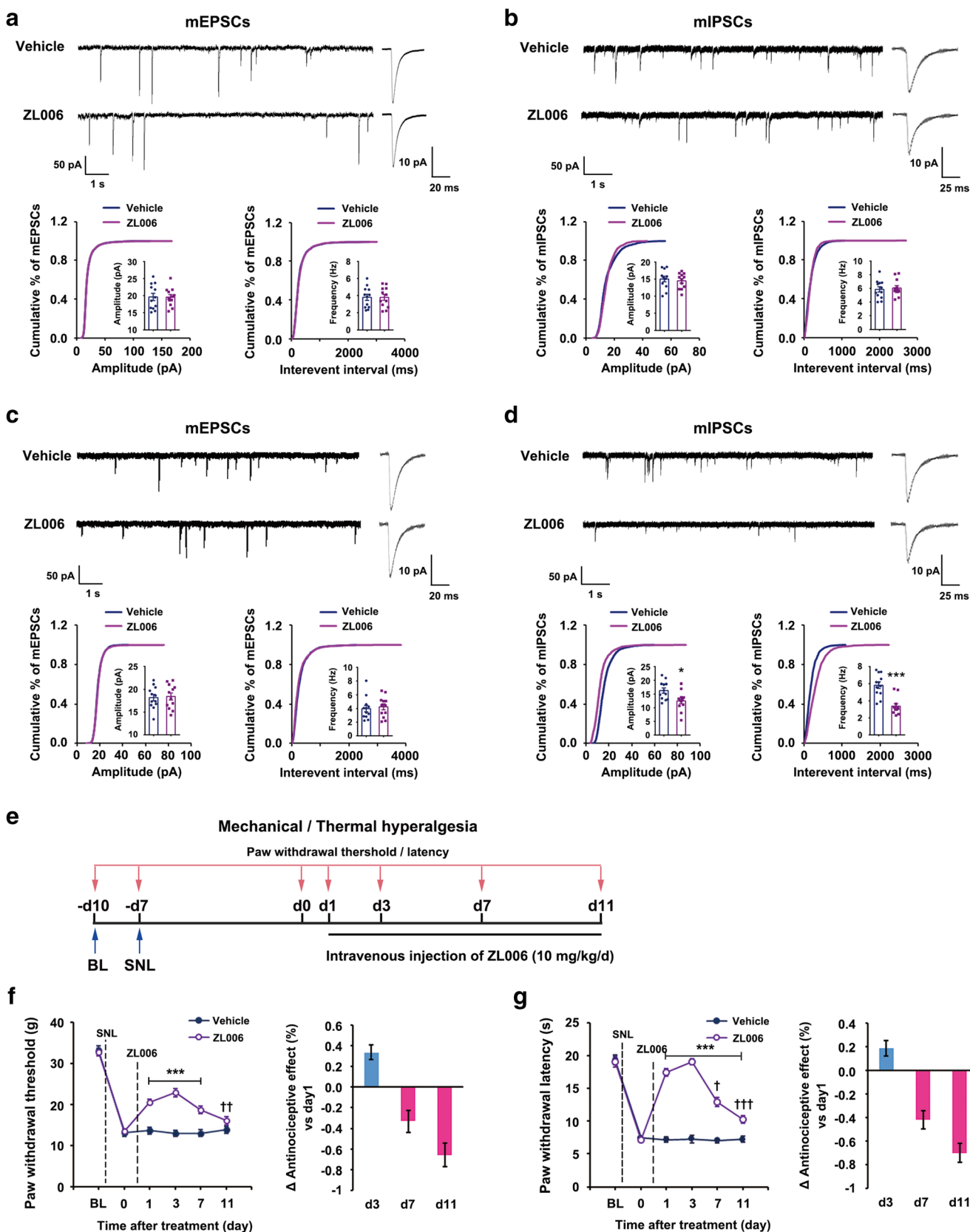
NO as a retrograde messenger signal potentiates presynaptic GABA release and inhibitory postsynaptic currents [36–38], and postsynaptic NMDAR activation at glutamate synapses potentiates GABA release at neighboring inhibitory nerve terminal [36], which can explain the alteration of the frequency of mIPSCs by the chronic use of NMDARs or PSD-95–nNOS inhibitor. However, how does PSD-95–nNOS–NO cascade change mIPSCs amplitude? To answer this, we treated rats with ZL006 (10 mg/kg/day, *i.v.*, a dose that produced > 90% maximal possible effect on paclitaxel-induced mechanical

**Fig. 3** Chronically uncoupling PSD-95–nNOS induces disinhibition and analgesic tolerance. **(a–d)** Recordings of mEPSCs and mIPSCs. Upper, representative (left) and averaged (right) traces of mPSCs. Lower, cumulative distribution plots and bar graph showing the amplitude (left) and frequency (right) of mPSCs. **(a)** Recordings of mEPSCs from acute spinal slices of rats incubated with ZL006 (1 µM) or vehicle for 30 min (for amplitude,  $F(1, 22) = 0.0392$ ,  $p = 0.98901$ ; for frequency,  $F(1, 22) = 0.0109$ ,  $p = 0.9914$ , 2-tailed  $t$  test,  $n = 12$ ). **(b)** Recordings of mIPSCs from acute spinal slices of rats incubated with ZL006 or vehicle for 30 min (for amplitude,  $F(1, 22) = 0.5081$ ,  $p = 0.6165$ ; for frequency,  $F(1, 22) = 0.3766$ ,  $p = 0.7101$ , 2-tailed  $t$  test,  $n = 12$ ). **(c)** Recordings of mEPSCs from acute spinal slices of rats that received intrathecal infusion of ZL006 (0.2 mg/kg/day × 11 days) (for amplitude,  $F(1, 22) = 0.2386$ ,  $p = 0.8084$ ; for frequency,  $F(1, 22) = 0.4022$ ,  $p = 0.6914$ , 2-tailed  $t$  test,  $n = 12$ ). **(d)** Recordings of mIPSCs from acute spinal slices of rats that received intrathecal infusion of ZL006 (for amplitude,  $F(1, 22) = 2.690$ ,  $p = 0.013$ ; for frequency,  $F(1, 22) = 5.194$ ,  $p = 3.297E-05$ , 2-tailed  $t$  test,  $n = 12$ ). All data are shown as mean ± SEM. **(e)** Design of experiments for **(f)** and **(g)**. **(f)** Left, mechanical hyperalgesia expressed as paw withdrawal threshold of rats subjected to the SNL surgery and treated with ZL006 or vehicle ( $F(1, 22) = 33.655$ , among groups: \*\*\* $p < 0.001$ , *vs* vehicle; within group: †† $p = 0.002$ , *vs* day 1, repeated measurements ANOVA,  $n = 12$ ). Right, the percent change of mechanical threshold for each subject. **(g)** Left, thermal hyperalgesia expressed as paw withdrawal latency of rats subjected to SNL surgery and treated with ZL006 or vehicle ( $F(1, 22) = 197.731$ , among groups: \*\*\* $p < 0.001$ , *vs* vehicle; within group: † $p = 0.013$ , ††† $p < 0.001$ , *vs* day 1, repeated measurements ANOVA,  $n = 12$ ). Right, the percent change of thermal threshold for each subject. Animals were treated with ZL006 (10 mg/kg/day, *i.v.*) for 11 days in **(f)** and **(g)**. All data are shown as mean ± SEM

allodynia) [11] for 1 or 11 days and measured GABA-evoked currents in the acute spinal cord slices. Though having similar median effective concentration ( $EC_{50}$ ) ( $100.03 \pm 1.096$  µM *vs*  $94.85 \pm 1.00$  µM), treatment with ZL006 for 11 days reduced maximal response ( $E_{max}$ ) of putative-excitatory neurons of laminae I in the dorsal horn to GABA by 41.5%, compared with treatment for 1 days ( $925.6 \pm 27.54$  pA *vs*  $1581.2 \pm 0.61$  pA) (Fig. 6a), indicating that chronic blockage of PSD-95–nNOS coupling causes the dysfunction of GABA<sub>A</sub>Rs.

To know how the PSD-95–nNOS–NO cascade affects the function of GABA<sub>A</sub>Rs, we measured the expression of BDNF, a member of the neurotrophin family of growth factors playing a predominant role in the initiation and maintenance of chronic pain [39]. It is reported that NO downregulates BDNF secretion and expression [40–42]. Chronic use of ZL006 significantly amplified the SNL-induced BDNF upregulation (Fig. 6b). Importantly, we treated rats with ZL006 (10 mg/kg/day, *i.v.*, × 11 days) with or without the BDNF scavenger TrkB-FC and found that TrkB-FC prevented ZL006 tolerance (Fig. 6 c and d). Similarly, TrkB receptor antagonist ANA-12 also prevented the ZL006 tolerance (Fig. 6 c and e). Therefore, BDNF upregulation may be responsible for the analgesic tolerance of ZL006.

BDNF is reported to inhibit the expression and function of KCC2, potassium-chloride cotransporter [43, 44]. Reduction in the activity of KCC2 in spinal lamina I neurons has been



implicated in neuropathic pain [45]. Moreover, the dysfunction of KCC2 shifts the chloride equilibrium potential ( $E_{Cl}$ ) to

a less negative value, resulting in that activation of GABA<sub>A</sub>Rs produces less hyperpolarization and less inhibition [43]. We

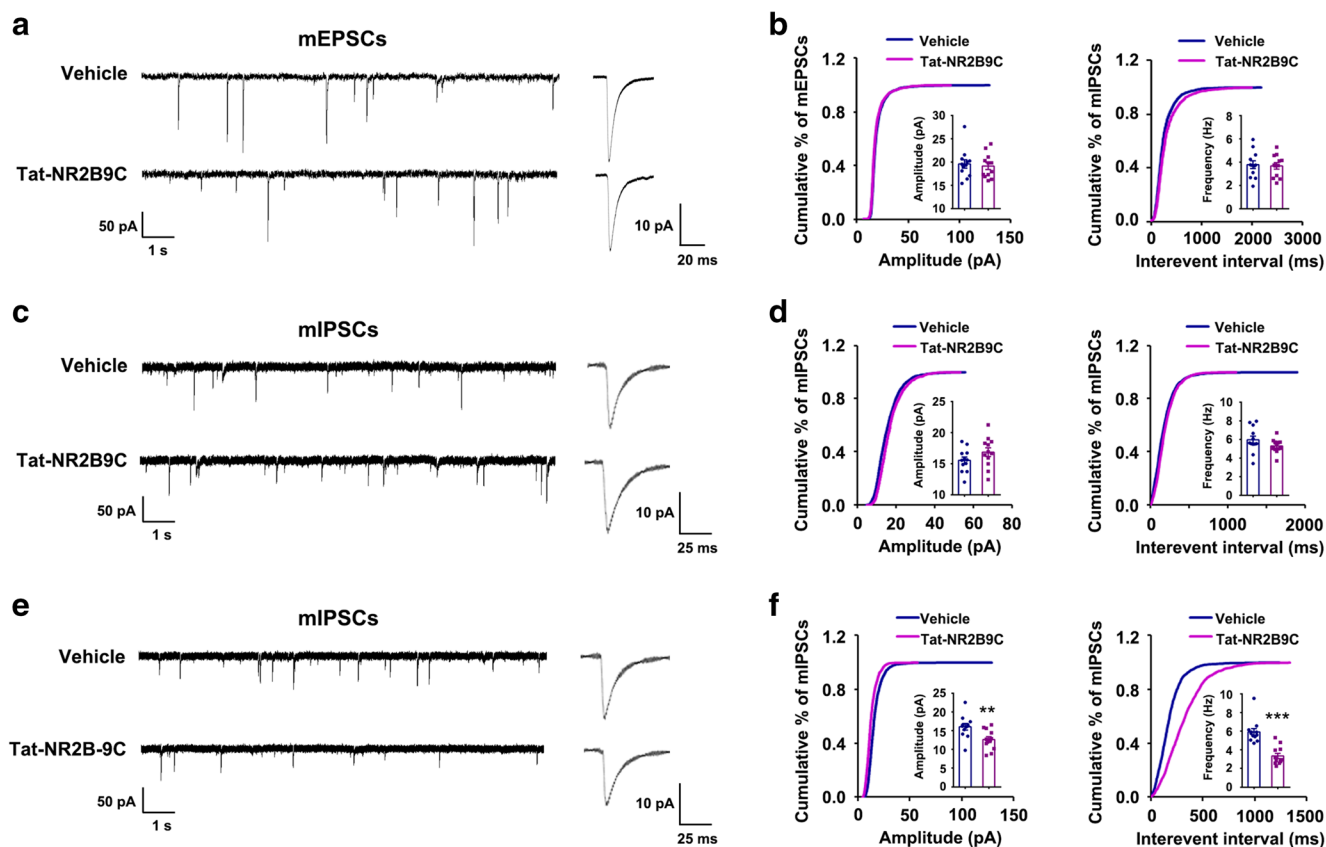


**Fig. 4** Chronic disassociation of PSD-95 from NR2B subunits of NMDARs induces disinhibition. (a–d) Recordings of mEPSCs and mIPSCs from acute spinal slices of rats incubated with Tat-NR2B9C (100 nM) or vehicle for 30 min. (a and c) Representative (left) and averaged (right) traces of mPSCs. (b and d) Cumulative distribution plots and bar graph showing the amplitude (left) and frequency (right) of mPSCs. In (b), for amplitude,  $F(1, 22) = 0.382$ ,  $p = 0.706$ ; for frequency,  $F(1, 22) = 0.245$ ,  $p = 0.809$ , 2-tailed  $t$  test,  $n = 12$ . In (d), for amplitude,  $F(1, 22) =$

1.501,  $p = 0.148$ ; for frequency,  $F(1, 22) = 1.487$ ,  $p = 0.151$ , 2-tailed  $t$  test,  $n = 12$ . (e–f) Recordings of mIPSCs from acute spinal slices of rats that received intrathecal microinjection of Tat-NR2B9C (0.5 pM/day, per animal,  $\times 11$  days). (e) Representative (left) and average (right) traces of mIPSCs. (f) Cumulative distribution plots and bar graph showing the amplitude (left) and frequency (right) of mIPSCs: for amplitude,  $F(1, 22) = 2.941$ ,  $**p = 0.0079$ ; for frequency,  $F(1, 22) = 5.648$ ,  $***p = 1.116E-05$ , 2-tailed  $t$  test,  $n = 12$ . All data are shown as mean  $\pm$  SEM

found that ZL006 significantly augmented SNL-induced decreases in both KCC2 and pKCC2 expression and ANA-12 reversed the downregulation of KCC2 by ZL006 (Fig. 6f). Together, the BDNF–KCC2 pathway may explain the GABA<sub>A</sub>R dysfunction and analgesic tolerance caused by the chronic disruption of the PSD-95–nNOS–NO cascade.

To further confirm that prolonged blockage of NMDARs induces analgesic tolerance through the BDNF–KCC2 pathway, we tested how MK801 affects the expression of BDNF and KCC2. The same as ZL006, the chronic use of MK801 also significantly amplified both the upregulation of BDNF and the reduction of KCC2 by SNL surgery (Fig. 7a and b). Besides, we verified the effect of TrkB-FC on the analgesic tolerance caused by prolonged blockage of NMDARs (Fig. 7c). Similarly, TrkB-FC also prevented the analgesic tolerance of MK801 (Fig. 7d). Together, chronic blockage of NMDARs induces analgesic tolerance through the NO–BDNF–KCC2 pathway.

In addition, both glial activation and extracellular signal-regulated kinase (ERK) phosphorylation are widely reported

to be associated with central sensitization [4, 44, 46, 47]. And we found that the expression of both Iba1 and GFAP in the spinal dorsal horn were markedly increased after SNL and further augmented after long-term treatment with MK801 (Fig. S3A and B), indicating the increased activation of microglial and astrocytes. This is also consistent with the expression of BDNF, as BDNF in the spinal dorsal horn is mainly released by activated microglial cells [4, 46]. The phosphorylation of ERK was also upregulated by SNL surgery, and in contrast, the chronic blockage of NMDARs had no effect on ERK phosphorylation (Fig. S3C).

## Discussion

Chronic neuropathic pain is a debilitating condition that remains challenging to treat [48, 49]. In the present study, we show here that nerve injury not only increased excitatory synaptic transmission but also reduced inhibition in putative-

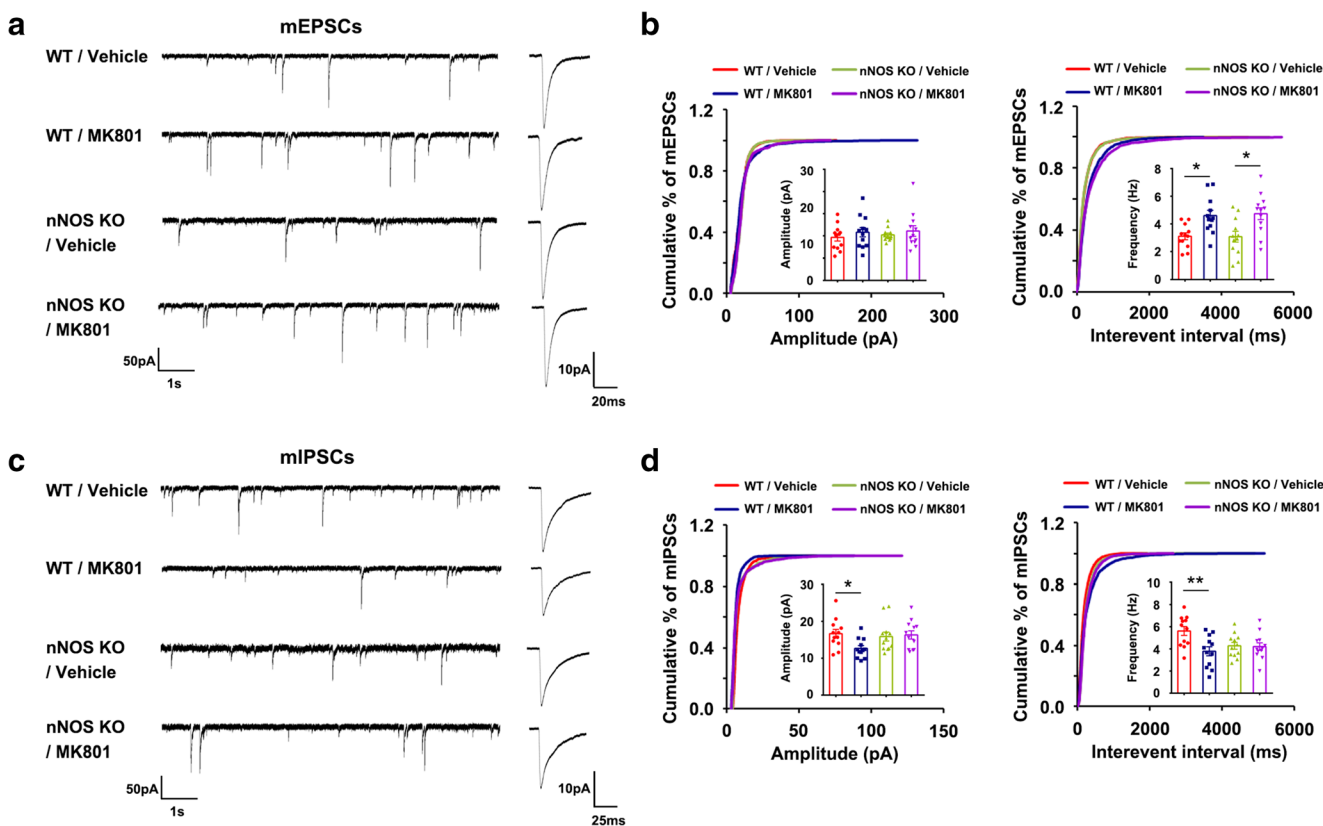


**Fig. 5** nNOS signal contributes to chronic blockage of NMDAR-induced disinhibition at the spinal level. (**a–d**) Recordings of mEPSCs and mIPSCs from acute spinal slices of nNOS KO and WT mice that received chronic intrathecal infusion of MK801 (2 µg/day × 11 days, per animal). (**a**) Representative (left) and averaged (right) traces of mEPSCs. (**b**) Cumulative distribution plots and bar graph showing the amplitude (left) and frequency (right) of mEPSCs: for amplitude,  $F(3, 44) = 0.431$ ,  $p = 0.732$ ; for frequency,  $F(3, 44) = 6.200$ , WT vehicle *versus* WT MK801:  $*p = 0.036$ , nNOS KO vehicle *versus* nNOS KO MK801:  $*p = 0.015$ , ANOVA,  $n = 12$ . (**c**) Representative (left) and averaged (right) traces of mIPSCs. (**d**) Cumulative distribution plots and bar graph showing the amplitude (left) and frequency (right) of mIPSCs: for amplitude,  $F(3, 44) = 2.929$ ,  $*p = 0.012$ ; for frequency,  $F(3, 44) = 4.668$ ,  $**p = 0.006$ , ANOVA,  $n = 12$ . All data are shown as mean ± SEM

excitatory neurons of laminae I in the dorsal horn, indicating a remarkable central sensitization at the spinal level. Very surprisingly, chronically blocking NMDARs aggravated the central sensitization and produced analgesic tolerance mainly due to the diminished GABAergic inhibitory synaptic transmission. Similarly, it is reported that repeated treatment with gabapentin (1 of the gabapentinoids) for 2 weeks in poststroke pain of rats resulted in complete analgesic tolerance [50]. Moreover, chronic morphine treatment produced a depression of GABAergic synaptic transmission [51]. Repeated cocaine exposure reduced the amplitude of GABA-mediated synaptic currents in VTA dopamine neurons [52]. Thus, it is widely accepted that diminished inhibition in pain neural circuits of the spinal dorsal horn is a major contributor to different chronic pain forms [53]. Together, prolonged single regulation of pain neural circuit by analgesics can cause central sensitization, especially disinhibition, and analgesic tolerance. In fact, it has been believed that drugs that affect multiple processes, rather than a single specific target, show the greatest promise for neuropathic pain treatment [18, 54, 55], which is consistent

with our findings. Interestingly, we found that preventing NO reduction-induced disinhibition through blocking the BDNF–KCC2 pathway could avoid the development of central sensitization and analgesic tolerance of MK801. Our findings provide the rationale for a novel strategy to treat neuropathic pain and to develop a new analgesic.

Reduced GABAergic synaptic transmission may be crucial for the analgesic-induced disinhibition. It is well known that NO as a retrograde messenger signal potentiates presynaptic GABA release [36–38, 56–58]. Blocking the NMDAR–PSD-95–nNOS cascade reduces NO production [22]. Thus, reduction in mIPSC frequency by the chronic use of NMDAR antagonist can be explained by the NO-dependent presynaptic GABA release mechanism. Furthermore, NO regulates AMPAR trafficking in the brain by S-nitrosylation of the AMPAR auxiliary subunits or other mechanisms [59–61]. In the spinal cord, there are presynaptic AMPA receptor subunits in GABAergic dorsal horn neurons. The presynaptic AMPA receptor activation enhances GABA release and mIPSC frequency in lamina I and II neurons [62]. It may be possible that

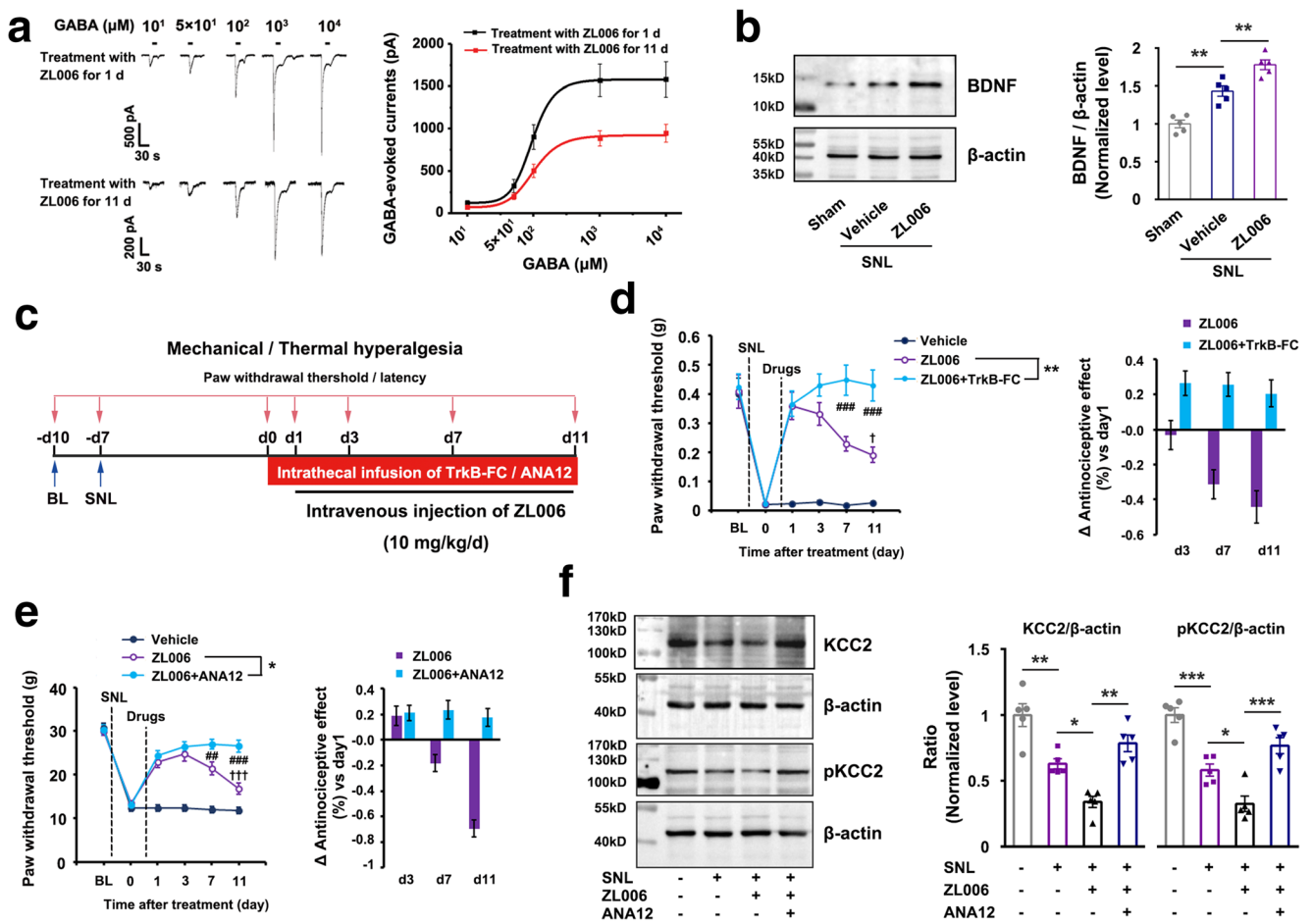


**Fig. 6** Chronic dissociation of PSD-95–nNOS causes GABA dysfunction through BDNF–KCC2 signaling. (a) Representative recordings (left) and dose/response plots of GABA-evoked currents (right) in the rats subjected to SNL and treated with ZL006 for 1 or 11 days,  $n = 12$ . (b) Immunoblots showing BDNF levels in the spinal dorsal horn of rats subjected to SNL surgery and treated with ZL006 (10 mg/kg/day or vehicle, i.v.,  $\times 11$  days,  $F(2, 12) = 40.642$ ,  $**p = 0.0012$ , vehicle vs sham;  $**p = 0.006$ , ZL006 vs vehicle, ANOVA,  $n = 5$ ). (c) Design of experiments for (d) and (e). (d) Left, effect of ZL006 (10 mg/kg/day, i.v.,  $\times 11$  days) with or without TrkB-FC (0.2 μg/day, per animal, intrathecal infusion using osmotic pump,  $\times 11$  days) in mice on SNL-induced mechanical hyperalgesia (among groups:  $F(2, 39) = 42.606$ , ZL006 + TrkB-FC vs ZL006:  $**p = 0.008$ ,  $###p < 0.001$ ; within the ZL006 group:  $†p = 0.035$ , day 11 vs day 1, repeated measurements ANOVA,  $n = 14$ ). Right, the percent change of thermal threshold for each subject. (e) Left, effect of

ZL006 with or without ANA-12 (3 μg/day, per animal, intrathecal infusion using osmotic pump,  $\times 11$  days) in rats on SNL-induced mechanical hyperalgesia (among groups:  $F(2, 39) = 33.518$ , ZL006 + ANA-12 vs ZL006:  $*p = 0.024$ ,  $##p = 0.006$ ,  $###p < 0.001$ ; within the ZL006 group:  $†††p < 0.001$ , day 11 vs day 1, repeated measurements ANOVA,  $n = 14$ ). Right, the percent change of thermal threshold for each subject. (f) Immunoblots showing the levels of KCC2 and pKCC2 in the spinal dorsal horn of rats treated by ZL006 (10 mg/kg/day, i.v.,  $\times 11$  days) with or without ANA-12 (3 μg/day, intrathecal infusion with osmotic pump). For KCC2,  $F(3, 16) = 20.848$ ,  $**p = 0.005$  (sham vs vehicle),  $*p = 0.032$  (vehicle vs ZL006),  $**p = 0.001$  (ZL006 vs ZL006 + ANA-12); for pKCC2,  $F(3, 16) = 26.447$ ,  $***p = 0.0008$  (sham vs vehicle),  $*p = 0.038$  (vehicle vs ZL006),  $***p = 0.0005$  (ZL006 vs ZL006 + ANA-12), ANOVA,  $n = 5$ . All data are shown as mean  $\pm$  SEM

NO indirectly promotes GABA release via presynaptic AMPA receptor. The postsynaptic actions of NO on GABA<sub>A</sub>Rs remain to be illuminated. NO downregulates BDNF secretion in cultured hippocampal neurons [41]. Here we showed that prolonged blockade of the NMDAR–PSD-95–nNOS cascade caused postsynaptic GABA<sub>A</sub>R dysfunction in putative excitatory dorsal horn neurons via the BDNF–KCC2 pathway. Both BDNF and KCC2 are crucial for the initiation and maintenance of chronic pain [39, 45]. In addition, it is reported that chronic blockade of NMDA receptors reduces GAD67 expression [63], which may also affect mIPSCs in part.

Interestingly, in general, NO induced by NMDAR activation in the spinal cord has been reported to induce or increase central sensitization and hyperalgesia. This seems to be contradictory to our finding that long-term NO reduction induced by NMDA receptor antagonist contributed to aggravation of central sensitization and analgesic tolerance. The different effects between short-term and lasting reductions of NO production may explain this discrepancy. Several mechanisms of hyperalgesia caused by NO have been reported, including cGMP formation, S-nitrosylation of target proteins, and Toll-like receptor activation and even directly amplifying the excitability of pain

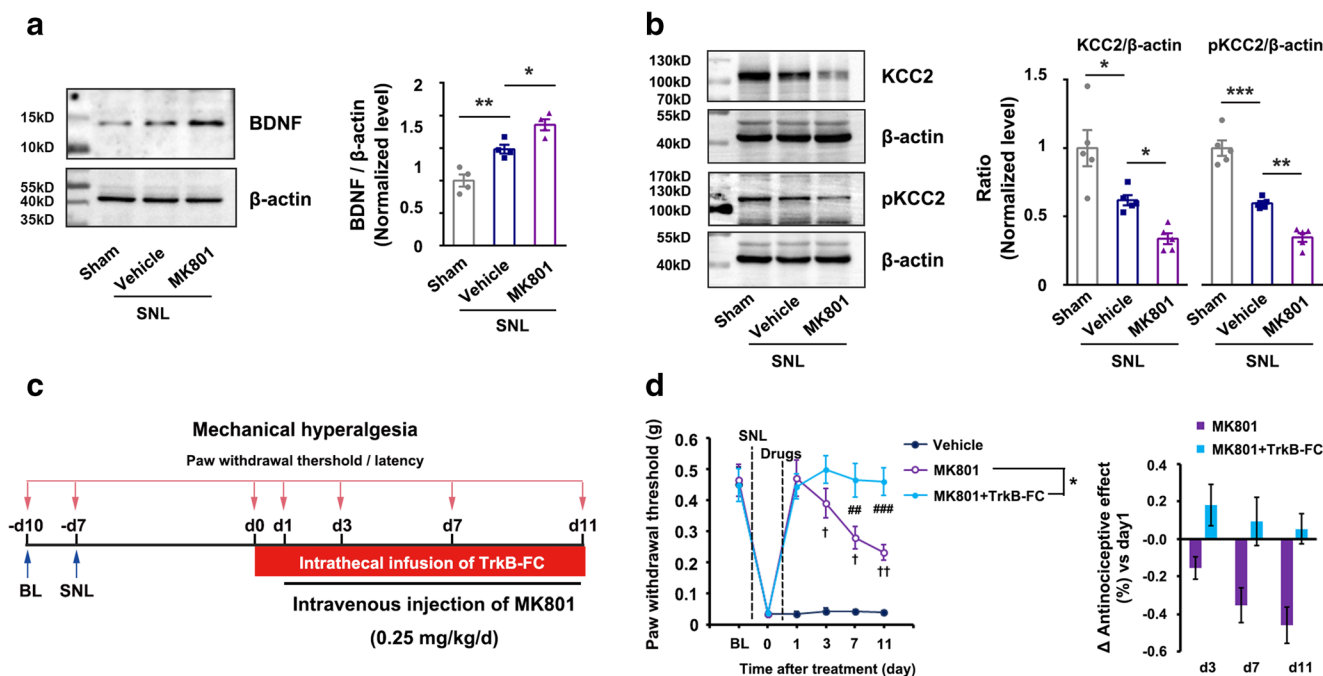


**Fig. 7** Chronic blockage of NMDARs causes analgesic tolerance through BDNF–KCC2 signaling. **(a)** Immunoblots showing BDNF levels in the spinal dorsal horn of rats subjected to SNL surgery and treated with MK801 (0.25 mg/kg/day or vehicle, i.v., × 11 days) ( $F(2, 9) = 26.972$ ,  $**p = 0.008$ , vehicle vs sham;  $*p = 0.033$ , ZL006 vs vehicle, ANOVA,  $n = 4$ ). **(b)** Immunoblots showing the levels of KCC2 and pKCC2 in the spinal dorsal horn of rats treated with MK801 (0.25 mg/kg/day or vehicle, i.v., × 11 days). For KCC2,  $F(2, 12) = 18.965$ ,  $*p = 0.019$  (sham vs vehicle),  $*p = 0.048$  (vehicle vs MK801); for pKCC2,  $F(3, 16) = 71.771$ ,

$***p < 0.001$  (sham vs vehicle),  $*p = 0.003$  (vehicle vs MK801), ANOVA,  $n = 5$ . **(c)** Design of the experiments for **(d)**. **(d)** Left, effect of MK801 (0.25 mg/kg/day or vehicle, i.v., × 11 days) with or without TrkB-FC (0.2 μg/day, per animal, intrathecal infusion using osmotic pump, × 11 days) in mice on SNL-induced mechanical hyperalgesia (among groups:  $F(2, 33) = 56.045$ , ZL006 + TrkB-FC vs ZL006:  $*p = 0.016$ ,  $###p < 0.001$ ; within the ZL006 group:  $†p = 0.035$ , day 11 vs day 1, repeated measurements ANOVA,  $n = 14$ ). Right, the percent change of thermal threshold for each subject. All data are shown as mean ± SEM

projection neurons [64–67], most of which are in a quick manner. Different from short-term NO reduction, however, lasting reduction of NO may affect central sensitization through a different signal pathway, such as glia activation, BDNF expression, and release from activated microglia cells and the following regulation on KCC2 expression and GABAARs, finally causing the amplified central sensitization and analgesic tolerance [41, 42, 44]. Moreover, the antinociceptive effect of NO at low levels may also partly cause the aggravation of central sensitization and analgesic tolerance after lasting reduction of NO production [64, 68, 69]. Besides, it has been observed that NO potentiates presynaptic GABA release and inhibitory postsynaptic currents [37, 38], which may also support our findings that a lasting reduction of NO production resulted in aggravation of central sensitization.

Besides disinhibition of pain neural circuit at the spinal level, chronic use of MK801 increased mEPSC frequency, suggesting they affect presynaptic glutamate release. NO reduces glutamate release from primary afferent fibers (PAFs) through S-nitrosylation of voltage-activated  $Ca^{2+}$  channels [70]. Long-lastingly reduced NO by the chronic use of MK801 may contribute to the mEPSC frequency increase. It is known that  $Ca^{2+}$ -dependent desensitization of postsynaptic NMDA receptor can

occur following  $Ca^{2+}$  entry through the NMDARs or through voltage-gated  $Ca^{2+}$  channels [71]. Central terminals of PAFs express NMDARs [72]. Chronic use of MK801 may sensitize presynaptic NMDARs and leads to glutamate release, which may explain mEPSC frequency increase. Understanding the mechanisms of increased mEPSC frequency by the chronic use of MK801 needs to be explored in the future.

## Conclusions

In this study, we demonstrate that prolonged use of the NMDAR antagonist MK801 does not prevent but promotes central sensitization and develops analgesic tolerance. The analgesic tolerance is mainly caused by reduced inhibitory synaptic transmission. The GABAergic disinhibition results from reduced NO production from nNOS, as NO reduction both decreases presynaptic GABA release and contributes to BDNF-mediated KCC2 dysfunction. Our studies also demonstrate that the tolerance of NMDAR antagonist can be prevented by blocking the BDNF–KCC2 pathway, which may provide a novel therapeutic approach for chronic neuropathic pain.

**Acknowledgments** This work was supported by grants from the National Natural Science Foundation of China (31530091, 81870912), National Key Research and Development Program of China (2016YFC1306703), and Science and Technology Program of Guangdong (2018B030334001) and by the Collaborative Innovation Center for Cardiovascular Disease Translational Medicine.

**Author Contributions** J. L. carried out the electrophysiological experiments in the acute spinal cord slices. F. L. synthesized target compounds. J. L., L. Z., and C. X. prepared pain models and performed the behavioral testing, Western blot, and coimmunoprecipitation works. Y. H. L., Y. Z., H. Y. W., L. C., Y. D. Z., and C. X. L. participated in the study. D. Y. Z. initiated the project, designed the study, and wrote the manuscript. All authors contributed to data analysis.

**Compliance with Ethical Standards** All procedures involving the use of animals were approved by the Institutional Animal Care and Use Committee of Nanjing Medical University.

**Conflict of Interest** The authors declare that they have no competing interests.

**Required Author Forms** [Disclosure forms](#) provided by the authors are available with the online version of this article.

## References

- Colloca L, Ludman T, Bouhassira D, et al. Neuropathic pain. *Nat Rev Dis Primers* 2017;3:17002.
- Attal N, Bouhassira D, Baron R. Diagnosis and assessment of neuropathic pain through questionnaires. *Lancet Neurol* 2018;17(5):456-66.
- van Hecke O, Austin SK, Khan RA, Smith BH, Torrance N. Neuropathic pain in the general population: a systematic review of epidemiological studies. *Pain*. 2014;155(4):654-62.
- Basbaum AI, Bautista DM, Scherrer G, Julius D. Cellular and molecular mechanisms of pain. *Cell*. 2009;139(2):267-84.
- Ji RR, Kohno T, Moore KA, Woolf CJ. Central sensitization and LTP: do pain and memory share similar mechanisms? *Trends Neurosci* 2003;26(12):696-705.
- Huang YJ, Lee KH, Murphy L, Garraway SM, Grau JW. Acute spinal cord injury (SCI) transforms how GABA affects nociceptive sensitization. *Exp Neurol*. 2016;285(Pt A):82-95.
- Tuchman M, Barrett JA, Donevan S, Hedberg TG, Taylor CP. Central sensitization and Ca(V)alpha(2)delta ligands in chronic pain syndromes: pathologic processes and pharmacologic effect. *J Pain* 2010;11(12):1241-9.
- Latremoliere A, Woolf CJ. Central sensitization: a generator of pain hypersensitivity by central neural plasticity. *J Pain* 2009;10(9):895-926.
- Kuner R. Central mechanisms of pathological pain. *Nat Med* 2010;16(11):1258-66.
- Cui WQ, Sun WS, Xu F, et al. Spinal serotonin 1A receptor contributes to the analgesia of acupoint catgut embedding by inhibiting phosphorylation of the N-methyl-D-aspartate receptor GluN1 subunit in complete Freund's adjuvant-induced inflammatory pain in rats. *J Pain*. 2019;20(1):16 e1-16 e16.
- Lee WH, Xu Z, Ashpole NM, et al. Small molecule inhibitors of PSD95-nNOS protein-protein interactions as novel analgesics. *Neuropharmacology*. 2015;97:464-75.
- Jorum E, Warncke T, Stubhaug A. Cold allodynia and hyperalgesia in neuropathic pain: the effect of N-methyl-D-aspartate (NMDA) receptor antagonist ketamine—a double-blind, cross-over comparison with alfentanil and placebo. *Pain*. 2003;101(3):229-35.
- Aiyer R, Mehta N, Gungor S, Gulati A. A systematic review of NMDA receptor antagonists for treatment of neuropathic pain in clinical practice. *Clin J Pain* 2018;34(5):450-67.
- Gagnon M, Bergeron MJ, Lavertu G, et al. Chloride extrusion enhancers as novel therapeutics for neurological diseases. *Nat Med* 2013;19(11):1524-8.
- Kim YH, Back SK, Davies AJ, et al. TRPV1 in GABAergic interneurons mediates neuropathic mechanical allodynia and disinhibition of the nociceptive circuitry in the spinal cord. *Neuron*. 2012;74(4):640-7.
- Peirs C, Seal RP. Neural circuits for pain: recent advances and current views. *Science*. 2016;354(6312):578-84.
- Polgar E, Sardella TC, Watanabe M, Todd AJ. Quantitative study of NPY-expressing GABAergic neurons and axons in rat spinal dorsal horn. *J Comp Neurol* 2011;519(6):1007-23.
- Alles SRA, Smith PA. Etiology and pharmacology of neuropathic pain. *Pharmacol Rev* 2018;70(2):315-47.
- Marsden KC, Beattie JB, Friedenthal J, Carroll RC. NMDA receptor activation potentiates inhibitory transmission through GABA receptor-associated protein-dependent exocytosis of GABA(A) receptors. *J Neurosci* 2007;27(52):14326-37.
- Zhang SY, Xu M, Miao QL, Poo MM, Zhang XH. Endocannabinoid-dependent homeostatic regulation of inhibitory synapses by miniature excitatory synaptic activities. *J Neurosci* 2009;29(42):13222-31.
- Chung JM, Kim HK, Chung K. Segmental spinal nerve ligation model of neuropathic pain. *Methods Mol Med* 2004;99:35-45.
- Zhou L, Li F, Xu HB, et al. Treatment of cerebral ischemia by disrupting ischemia-induced interaction of nNOS with PSD-95. *Nat Med* 2010;16(12):1439-43.
- Luo CX, Lin YH, Qian XD, et al. Interaction of nNOS with PSD-95 negatively controls regenerative repair after stroke. *J Neurosci* 2014;34(40):13535-48.
- Zhou HH, Tang Y, Zhang XY, et al. Delayed administration of Tat-HA-NR2B9c promotes recovery after stroke in rats. *Stroke*. 2015;46(5):1352-8.
- Corder G, Tawfik VL, Wang D, et al. Loss of mu opioid receptor signaling in nociceptors, but not microglia, abrogates morphine tolerance without disrupting analgesia. *Nat Med* 2017;23(2):164-73.
- Ramer LM, McPhail LT, Borisoff JF, et al. Endogenous TrkB ligands suppress functional mechanosensory plasticity in the deafferented spinal cord. *J Neurosci* 2007;27(21):5812-22.
- Chaplan SR, Bach FW, Pogrel JW, Chung JM, Yaksh TL. Quantitative assessment of tactile allodynia in the rat paw. *J Neurosci Methods* 1994;53(1):55-63.
- Yasaka T, Tiong SY, Hughes DI, Riddell JS, Todd AJ. Populations of inhibitory and excitatory interneurons in lamina II of the adult rat spinal dorsal horn revealed by a combined electrophysiological and anatomical approach. *Pain*. 2010;151(2):475-88.
- Punnakkal P, von Schoultz C, Haenraets K, Wildner H, Zeilhofer HU. Morphological, biophysical and synaptic properties of glutamatergic neurons of the mouse spinal dorsal horn. *J Physiol* 2014;592(4):759-76.
- Lu VB, Biggs JE, Stebbing MJ, et al. Brain-derived neurotrophic factor drives the changes in excitatory synaptic transmission in the rat superficial dorsal horn that follow sciatic nerve injury. *J Physiol* 2009;587(Pt 5):1013-32.
- Walters RJ, Hadley SH, Morris KD, Amin J. Benzodiazepines act on GABAA receptors via two distinct and separable mechanisms. *Nat Neurosci* 2000;3(12):1274-81.
- Schwartz PH, Wasterlain CG. Cardiac arrest and resuscitation alters the pharmacokinetics of MK-801 in the rat. *Res Commun Chem Pathol Pharmacol* 1991;73(2):181-95.

33. Wong EH, Kemp JA, Priestley T, Knight AR, Woodruff GN, Iversen LL. The anticonvulsant MK-801 is a potent N-methyl-D-aspartate antagonist. *Proc Natl Acad Sci U S A* 1986;83(18):7104-8.
34. Carey LM, Lee WH, Gutierrez T, et al. Small molecule inhibitors of PSD95-nNOS protein-protein interactions suppress formalin-evoked Fos protein expression and nociceptive behavior in rats. *Neuroscience*. 2017;349:303-17.
35. Lai TW, Wang YT. Fashioning drugs for stroke. *Nat Med* 2010;16(12):1376-8.
36. Nugent FS, Penick EC, Kauer JA. Opioids block long-term potentiation of inhibitory synapses. *Nature*. 2007;446(7139):1086-90.
37. Fenselau H, Heinke B, Sandkuhler J. Heterosynaptic long-term potentiation at GABAergic synapses of spinal lamina I neurons. *J Neurosci* 2011;31(48):17383-91.
38. Hardingham N, Dachtler J, Fox K. The role of nitric oxide in presynaptic plasticity and homeostasis. *Front Cell Neurosci* 2013;7:190.
39. Beggs S, Trang T, Salter MW. P2X4R+ microglia drive neuropathic pain. *Nat Neurosci* 2012;15(8):1068-73.
40. Xiong H, Yamada K, Han D, et al. Mutual regulation between the intercellular messengers nitric oxide and brain-derived neurotrophic factor in rodent neocortical neurons. *Eur J Neurosci* 1999;11(5):1567-76.
41. Canossa M, Giordano E, Cappello S, Guamieri C, Ferri S. Nitric oxide down-regulates brain-derived neurotrophic factor secretion in cultured hippocampal neurons. *Proc Natl Acad Sci U S A* 2002;99(5):3282-7.
42. Hsieh HY, Robertson CL, Vermehren-Schmaedick A, Balkowiec A. Nitric oxide regulates BDNF release from nodose ganglion neurons in a pattern-dependent and cGMP-independent manner. *J Neurosci Res* 2010;88(6):1285-97.
43. Coull JA, Beggs S, Boudreau D, et al. BDNF from microglia causes the shift in neuronal anion gradient underlying neuropathic pain. *Nature*. 2005;438(7070):1017-21.
44. Ferrini F, De Koninck Y. Microglia control neuronal network excitability via BDNF signalling. *Neural Plast* 2013;2013:429815.
45. Mapplebeck JCS, Lorenzo LE, Lee KY, et al. Chloride dysregulation through downregulation of KCC2 mediates neuropathic pain in both sexes. *Cell Rep* 2019;28(3):590-96 e4.
46. Inoue K, Tsuda M. Microglia in neuropathic pain: cellular and molecular mechanisms and therapeutic potential. *Nat Rev Neurosci* 2018;19(3):138-52.
47. Hu HJ, Carrasquillo Y, Karim F, et al. The kv4.2 potassium channel subunit is required for pain plasticity. *Neuron*. 2006;50(1):89-100.
48. Kuner R, Flor H. Structural plasticity and reorganisation in chronic pain. *Nat Rev Neurosci* 2017;18(2):113.
49. Ligon CO, Moloney RD, Greenwood-Van Meerveld B. Targeting epigenetic mechanisms for chronic pain: a valid approach for the development of novel therapeutics. *J Pharmacol Exp Ther* 2016;357(1):84-93.
50. Yang F, Fu H, Lu YF, et al. Post-stroke pain hypersensitivity induced by experimental thalamic hemorrhage in rats is region-specific and demonstrates limited efficacy of gabapentin. *Neurosci Bull* 2014;30(6):887-902.
51. Wilson-Poe AR, Jeong HJ, Vaughan CW. Chronic morphine reduces the readily releasable pool of GABA, a presynaptic mechanism of opioid tolerance. *J Physiol* 2017;595(20):6541-55.
52. Liu QS, Pu L, Poo MM. Repeated cocaine exposure in vivo facilitates LTP induction in midbrain dopamine neurons. *Nature*. 2005;437(7061):1027-31.
53. Knabl J, Witschi R, Hosl K, et al. Reversal of pathological pain through specific spinal GABAA receptor subtypes. *Nature*. 2008;451(7176):330-4.
54. Gadotti VM, Bladen C, Zhang FX, et al. Analgesic effect of a broad-spectrum dihydropyridine inhibitor of voltage-gated calcium channels. *Pflugers Arch* 2015;467(12):2485-93.
55. Zamponi GW, Striessnig J, Koschak A, Dolphin AC. The physiology, pathology, and pharmacology of voltage-gated calcium channels and their future therapeutic potential. *Pharmacol Rev* 2015;67(4):821-70.
56. Szabadits E, Cserep C, Ludanyi A, et al. Hippocampal GABAergic synapses possess the molecular machinery for retrograde nitric oxide signaling. *J Neurosci* 2007;27(30):8101-11.
57. Tarasenko A, Krupko O, Himmelreich N. New insights into molecular mechanism(s) underlying the presynaptic action of nitric oxide on GABA release. *Biochim Biophys Acta* 2014;1840(6):1923-32.
58. Maddox JW, Gleason E. Nitric oxide promotes GABA release by activating a voltage-independent Ca(2+) influx pathway in retinal amacrine cells. *J Neurophysiol* 2017;117(3):1185-99.
59. Huang Y, Man HY, Sekine-Aizawa Y, et al. S-nitrosylation of N-ethylmaleimide sensitive factor mediates surface expression of AMPA receptors. *Neuron*. 2005;46(4):533-40.
60. Serulle Y, Zhang S, Ninan I, et al. A GluR1-cGKII interaction regulates AMPA receptor trafficking. *Neuron*. 2007;56(4):670-88.
61. Selvakumar B, Haganir RL, Snyder SH. S-nitrosylation of stargazin regulates surface expression of AMPA-glutamate neurotransmitter receptors. *Proc Natl Acad Sci U S A* 2009;106(38):16440-5.
62. Engelmann HS, Anderson RL, Daniele C, Macdermott AB. Presynaptic alpha-amino-3-hydroxy-5-methyl-4-isoxazolepropionic acid (AMPA) receptors modulate release of inhibitory amino acids in rat spinal cord dorsal horn. *Neuroscience*. 2006;139(2):539-53.
63. Kinney JW, Davis CN, Tabarean I, Conti B, Bartfai T, Behrens MM. A specific role for NR2A-containing NMDA receptors in the maintenance of parvalbumin and GAD67 immunoreactivity in cultured interneurons. *J Neurosci* 2006;26(5):1604-15.
64. Schmidtke A. Nitric oxide-mediated pain processing in the spinal cord. *Handb Exp Pharmacol* 2015;227:103-17.
65. Besson JM. The neurobiology of pain. *Lancet*. 1999;353(9164):1610-5.
66. Kim D, Kim MA, Cho IH, et al. A critical role of toll-like receptor 2 in nerve injury-induced spinal cord glial cell activation and pain hypersensitivity. *J Biol Chem* 2007;282(20):14975-83.
67. Obata K, Katsura H, Miyoshi K, et al. Toll-like receptor 3 contributes to spinal glial activation and tactile allodynia after nerve injury. *J Neurochem* 2008;105(6):2249-59.
68. Paoloni JA, Appleyard RC, Nelson J, Murrell GA. Topical nitric oxide application in the treatment of chronic extensor tendinosis at the elbow: a randomized, double-blinded, placebo-controlled clinical trial. *Am J Sports Med* 2003;31(6):915-20.
69. Kina VA, Villarreal CF, Prado WA. The effects of intraspinal L-NOARG or SIN-1 on the control by descending pathways of incisional pain in rats. *Life Sci* 2005;76(17):1939-51.
70. Jin XG, Chen SR, Cao XH, Li L, Pan HL. Nitric oxide inhibits nociceptive transmission by differentially regulating glutamate and glycine release to spinal dorsal horn neurons. *J Biol Chem* 2011;286(38):33190-202.
71. Legendre P, Rosenmund C, Westbrook GL. Inactivation of NMDA channels in cultured hippocampal neurons by intracellular calcium. *J Neurosci* 1993;13(2):674-84.
72. Bardoni R. Role of presynaptic glutamate receptors in pain transmission at the spinal cord level. *Curr Neuropharmacol* 2013;11(5):477-83.

**Publisher's Note** Springer Nature remains neutral with regard to jurisdictional claims in published maps and institutional affiliations.